Acta Cardiol Sin 2016;32:65−74
Original Article
doi: 10.6515/ACS20150424G

Basic Science

Half-Logistic Function Model for First Half of Descending Phase of Cardiomyocyte Cytoplasmic Ca^{2+} Concentration ($[Ca^{2+}]_i$)-Time Curve (CaTCIII) in Isolated Aequorin-Injected Mouse Left Ventricular Papillary Muscle

Ju Mizuno,[1,2,3,4] Mikiya Otsuji,[1] Takeshi Yokoyama,[1,3] Hideko Arita[1,4] and Kazuo Hanaoka[1,4]

Background: Myocardial contraction and relaxation are regulated by increases and decreases in cytoplasmic calcium concentration ($[Ca^{2+}]_i$). In previous studies, we found that a half-logistic (h-L) function, which represents a half-curve of a symmetrical sigmoid logistic function with a boundary at the inflection point, curve-fits the first half of the ascending phase and the second half of the descending phase of the $[Ca^{2+}]_i$ transient curve better than a mono-exponential (m-E) function. In the present study, we investigated the potential application of an h-L function to analyse the first half of the descending phase of CaTC (CaTCIII).

Methods: The $[Ca^{2+}]_i$ was measured using the Ca^{2+}-sensitive aequorin, which was microinjected into 15 isolated mouse left ventricular (LV) papillary muscles. The observed CaTCIII data in the interval from the point corresponding to the peak $[Ca^{2+}]_i$ to the point corresponding to dCa/dt_{min} was curve-fitted using the h-L and m-E function equations by the least-squares method.

***Results*:** The mean correlation coefficient (r) values of the h-L and m-E function best curve-fits for 11 CaTCIIIs were 0.9986 and 0.9982, respectively. The Z transformation of h-L r (3.64 ± 0.45) was larger than that of m-E r (3.50 ± 0.33) ($p < 0.05$).

Conclusions: The h-L function can evaluate most CaTCIIIs more accurately than the m-E function in isolated aequorin-injected mouse LV papillary muscle. The three calculated h-L parameters i.e., amplitude constant, time constant, and non-zero asymptote, are more reliable indices than m-E for evaluating the magnitude and time course of the change in the decrease in $[Ca^{2+}]_i$.

Key Words: Ca^{2+} transient • Half-logistic amplitude constant • Half-logistic non-zero asymptote • Half-logistic time constant • Myocardial Ca^{2+} handling

INTRODUCTION

It is well-established that mammalian cardiac contraction and relaxation are regulated by increases and decreases in cardiomyocyte cytoplasmic free calcium (Ca^{2+}) concentration ($[Ca^{2+}]_i$) in myocardial Ca^{2+} handling and excitation-contraction (E-C) coupling.[1] The waveforms of the $[Ca^{2+}]_i$ transient provide valuable information for evaluating the change in $[Ca^{2+}]_i$.

Non-linear regression analyses with the least-squares method are valuable tools for elucidating the me-

Received: March 17, 2014 Accepted: April 24, 2015
[1]Department of Anesthesiology, Faculty of Medicine, The University of Tokyo, Tokyo 113-8549; [2]Department of Anesthesiology and Pain Medicine, Juntendo University Faculty of Medicine, Tokyo 113-8431; [3]Department of Dental Anesthesiology, Faculty of Dental Science, Kyushu University, Fukuoka 812-8582; [4]Department of Anesthesiology and Pain Relief Center, JR Tokyo General Hospital, Tokyo 151-8528, Japan.
Address correspondence and reprint requests to: Dr. Ju Mizuno, Department of Anesthesiology and Pain Medicine, Juntendo University Faculty of Medicine, 3-1-3 Hongo, Bunkyo-ku, Tokyo 113-8431, Japan. Tel: +81-3-3813-3111; Fax: +81-3-5689-3820; E-mail: mizuno_ju8@yahoo.co.jp

chanism, summarizing information, eliminating noise, allowing speculation regarding unmeasured data, and separating the effects of multiple factors. To maximize the amount of useful information extracted from the $[Ca^{2+}]_i$-time curve (CaTC), CaTC is generally divided into two sequential phases with a boundary at the peak $[Ca^{2+}]_i$ i.e., the ascending phase and the descending phase, which are regarded as the contraction and relaxation phases, respectively. However, the cardiac cycle does not suddenly alternate its contraction phase with its relaxation phase at one particular point; for example, the peak $[Ca^{2+}]_i$ and the contraction and relaxation phases have temporally overlapping phases. Therefore, the entire ascending phase is not the simple contraction process, and the entire descending phase is not the simple relaxation process.

Therefore, we need to investigate CaTC more thoroughly to understand contraction and relaxation functions, and the relationship between contraction and relaxation. We previously divided CaTC into four partial phases, with boundaries at three meaningful points i.e., the maximum of the first-order time derivative of $[Ca^{2+}]_i$ (dCa/dt_{max}), the peak $[Ca^{2+}]_i$, and the minimum of the first-order time derivative of $[Ca^{2+}]_i$ (dCa/dt_{min}), as shown in Figure 1: the first half of the ascending phase (CaTCI),[2] the second half of the ascending phase (CaTCII),[3] the first half of the descending phase (CaTCIII), and the second half of the descending phase of CaTC (CaTCIV).[4]

Furthermore, we curve-fitted the partial phases of CaTC with a half-logistic (h-L) function, which is a half-curve of a symmetrical sigmoid logistic function with a boundary at the inflection point, and obtained more information than when analyzing for the two sequential phases of CaTC. First, we found that the h-L time constant of CaTCI ($Ca\tau_{1L}$) represents the duration of the increase in $[Ca^{2+}]_i$ from the sarcoplasmic reticulum (SR) by Ca^{2+}-induced Ca^{2+} release (CICR) during the early part of the contraction process.[2] Secondly, we found that the h-L time constant of CaTCIV ($Ca\tau_{4L}$) represents the duration of the decrease in $[Ca^{2+}]_i$ resulting from Ca^{2+} sequestration into SR, and Ca^{2+} removal from the cytoplasm to the extracellular space through the Na^+/Ca^{2+} exchanger during the late part of the relaxation process.[4] Probably, CaTCII affects both the middle part of the contraction process and the early part of the relaxation process, and CaTCIII affects both the late part of the contraction process and the middle part of the relaxation process. Thereafter, we also demonstrated that CaTCII can be represented by the h-L function.[3] Therefore, unanalyzed CaTCIII may also be represented by the h-L function.

In the present study, we investigated the potential application of the h-L function to the analysis of CaTCIII in cardiomyocytes and sought to determine whether the h-L function curve-fits CaTCIII more accurately than the mono-exponential (m-E) function. An appropriate curve-fit for CaTCIII using the h-L function would provide three more reliable h-L function parameters, and increase our understanding of the combination of the late part of the contraction process and the middle part of the relaxation process in myocardial Ca^{2+} handling and E-C coupling.

MATERIALS AND METHODS

This study protocol was approved by the Animal Investigation Committee of the Jikei University School of Medicine. All procedures during the experiments were conducted in the Jikei University School of Medicine in conformity with the "Guiding Principles for the Care and Use of Animals in the Field of Physiological Sciences" endorsed by the American Physiological Society and the Physiological Society of Japan.

Surgical preparation

The experimental procedures of our study have been previously described in detail.[2-4] In short, 15 mice (C57BL/6; body weight 25-30 g) were anesthetized with intravenous (1.5-2.0 mg/kg) and intraperitoneal (15-20 mg/kg) pentobarbital sodium, respectively. Following removal of the heart, the aorta was cannulated with a blunted 18 G needle, and the heart was mounted on a Langendorff apparatus. The coronary blood was washed out with Tyrode's solution containing 2 mM Ca^{2+} buffered by *N*-2-hydroxyethyl-piperazine-*N*-2-ethanesulfonic acid (HEPES) at a constant pressure for 5 min. The solution was changed to HEPES-buffered Tyrode's solution containing 2 mM Ca^{2+} and 20 mM 2, 3-butanedione monoxime (BDM) after the heart beat was stabilized. Once the contraction stopped completely, the heart was removed from the Langendorff apparatus. A thin papillary muscle was dissected out from the mouse left ventricular (LV) walls. The muscle length and diameter of

the 15 isolated mouse LV papillary muscle specimens were 2.01 ± 0.43 and 0.63 ± 0.11 mm, respectively.

After both ends of the isolated muscle had been tied with silk thread, the muscle was mounted horizontally in an experimental chamber, immersed in a bath and continuously perfused with Tyrode's solution. One end of the muscle was attached to a fixed hook and the other was attached to the arm of a tension transducer (BG-10; Kulite Semiconductor Products, Leonia, NJ, USA; compliance 2.5 μm/g, unloaded resonant frequency 0.6 kHz). A pair of platinum black electrodes was placed parallel to the muscle, which was regularly stimulated by a single square pulse of 5 ms duration and 0.2 Hz; the strength of the stimulation was 1.5-fold the threshold. The muscle was slowly stretched and adjusted to the length at which the developed tension reached maximum (L_{max}).

Aequorin injection

Aequorin was dissolved in 150 mM KCl and 5 mM HEPES, pH 7.0, at a final concentration of 50-100 μM. Using glass micropipettes with a resistance of 30-50 MΩ, we injected aequorin into 150-200 superficial cells of the preparation using nitrogen gas. Aequorin light signals were detected using a photomultiplier (EMI 9789A; Thorn EMI, Ruislip, UK) placed just above the muscle.[5] In twitch response, the aequorin light signal was recorded through a 500-Hz low-pass filter. Sixty-four aequorin light signals were averaged to improve the signal-to-noise ratio.

The measurement of aequorin's light signal was essentially similar to those noted in previous reports.[6,7] Aequorin light signals were converted to $[Ca^{2+}]_i$ using an *in vitro* calibration curve.[8] The constants used in the present experiment were as follows: n, 3.14; K_R, 4,025,000; K_{TR}, 114.6.[9] Ca^{2+} signals were sampled at 1-ms intervals and digitized with an A/D converter. All Ca^{2+} data were stored on tape (NFR-3515W; Sony Magnescale, Tokyo, Japan) and a computer (PC-9801; NEC, Tokyo, Japan) for later analysis.

Tyrode's solution

Tyrode's solution buffered with HEPES was used during all experiments, including muscle dissection and aequorin injection. The composition of the solution (in mM) was as follows: NaCl, 136.9; KCl, 5.4; $MgCl_2$, 0.5; NaH_2PO_4, 0.33; HEPES, 5; glucose, 5. The pH was adjusted to 7.40 ± 0.05 with NaOH at 24 °C, and the solution was equilibrated with 100% O_2. The temperature of the solution was continuously monitored with a thermocouple and maintained at 30 ± 0.5 °C.

Ca^{2+} transient

Ca^{2+} signals were measured from the point before the twitch stimulation procedure was started. The Ca^{2+} signal gradually increased, reached a peak, then decreased and returned to the resting state before the following twitch stimulation – all within the 1,000-ms sampling window. Signals for CaTCIII, which extends from the point corresponding to the peak $[Ca^{2+}]_i$ data to the point corresponding to the dCa/dt_{min} data, as shown in Figure 1, were used for subsequent analyses. The dCa/dt was obtained by differentiating the sampled $[Ca^{2+}]_i$ data after digital smoothing using an 11-point, non-weighted moving average of digitized $[Ca^{2+}]_i$ data signals.

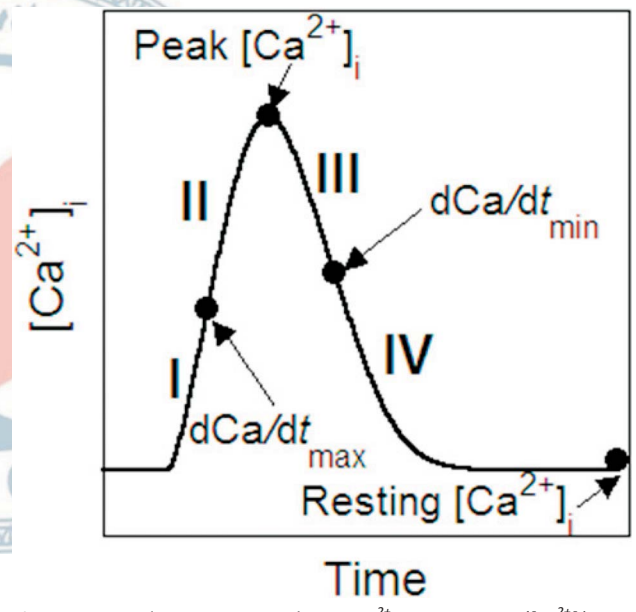

Figure 1. *Cardiomyocyte cytoplasmic Ca^{2+} concentration ($[Ca^{2+}]_i$)-time curve (CaTC) schema. The CaTC is divided into four partial phases with boundaries at three meaningful points, i.e., the maximum of the first-order time derivative of $[Ca^{2+}]_i$ (dCa/dt_{max}), the peak $[Ca^{2+}]_i$, and the minimum of the first-order time derivative of $[Ca^{2+}]_i$ (dCa/dt_{min}). The first half of the ascending phase of the CaTC (CaTCI) is the curve from the point corresponding to the beginning of twitch stimulation to the point corresponding to dCa/dt_{max}. The second half of the ascending phase of the CaTC (CaTCII) is the curve from the point corresponding to dCa/dt_{max} to the point corresponding to the peak $[Ca^{2+}]_i$. The first half of the descending phase of the CaTC (CaTCIII) is the curve from the point corresponding to the peak $[Ca^{2+}]_i$ to the point corresponding to dCa/dt_{min}. The second half of the descending phase of the CaTC (CaTCIV) is the curve from the point corresponding to dCa/dt_{min} to the point corresponding to the resting $[Ca^{2+}]_i$.*

h-L function equation

The following h-L function was used to curve-fit CaTCIII data by the least-squares method as shown in Figure 2A.

$$Ca(t) = 2Ca_{3A}/\{1 + \exp[-(t - t_{dC})/Ca\tau_{3L}]\} + Ca_{3B} \quad \text{(Eq. 1)}$$

where t is the time from the beginning of twitch stimulation to the point corresponding to the $[Ca^{2+}]_i$, Ca_{3A} is the h-L amplitude constant of CaTCIII, $Ca\tau_{3L}$ is the h-L time constant of CaTCIII, Ca_{3B} is the h-L non-zero asymptote of CaTCIII, and t_{dC} is a constant which represents the time at the point corresponding to dCa/dt_{min}. It is noted that t_{dC} is determined before the h-L function curve fitting. The h-L function curve given by Eq. 1 decreases monotonically from $Ca(-\infty)$ [= Ca_{3B}] to $Ca(t_{dC})$ [= $(Ca_{3A} + Ca_{3B})$]. $Ca\tau_{3L}$ value corresponds to the duration for the curves to decrease from $Ca(t_{dC} - Ca\tau_{3L})$ {= $[2Ca_{3A}/(1 + e) + Ca_{3B}]$ ~ $(0.54\ Ca_{3A} + Ca_{3B})$} to $Ca(t_{dC})$ [= $(Ca_{3A} + Ca_{3B})$].

m-E function equation

A m-E function was also used to curve-fit CaTCIII data by the least-squares method as shown in Figure 2B.

$$Ca(t) = Ca_{30}\exp[(t - t_{dC})/Ca\tau_{3E}] + Ca_{3\infty} \quad \text{(Eq. 2)}$$

where t is the time from the beginning of twitch stimulation to the point corresponding to the $[Ca^{2+}]_i$, Ca_{30} is the m-E amplitude constant of CaTCIII, $Ca\tau_{3E}$ is the m-E time constant of CaTCIII, $Ca_{3\infty}$ is the m-E function non-zero asymptote of CaTCIII, and t_{dC} is a constant which represents the time at the point corresponding to dCa/dt_{min}. It is noted that t_{dC} is determined before the m-E curve fitting. The m-E function curve given by Eq. 2 decreases monotonically from $Ca(-\infty)$ [= $Ca_{3\infty}$] to $Ca(t_{dC})$ [= $(Ca_{30} + Ca_{3\infty})$]. The $Ca\tau_{3E}$ value corresponds to the duration for the curve to decrease from $Ca(t_{dC} - Ca\tau_{3E})$ [= $(Ca_{30}/e + Ca_{3\infty})$ ~ $(0.37\ Ca_{30} + Ca_{3\infty})$] to $Ca(t_{dC})$ [= $(Ca_{30} + Ca_{3\infty})$].

It should be noted that the h-L function (Eq. 1) has the same number of variable parameters, -three- as the m-E function (Eq. 2), and that Ca_{3A}, $Ca\tau_{3L}$, and Ca_{3B} in Eq. 1 are conceptually similar to Ca_{30}, $Ca\tau_{3E}$, and $Ca_{3\infty}$ in Eq. 2, respectively.

Statistical analysis

Goodness of fit was evaluated with the correlation coefficient (r) and residual mean square (RMS) for the h-L and m-E curve-fitting models. Fisher's Z transformation (Z) of r[10] was calculated with the following equation: $Z = 1/2[\ln(1 + r) - \ln(1 - r)]$. Residual values were calculated as the observed $[Ca^{2+}]_i$ data during CaTCIII minus the best-fit h-L or m-E value at each sampling time point. RMS was calculated as the residual sum of squares (RSS) divided by the residual degrees of freedom, which indicates the number of data points analyzed minus the number of parameters in the function.[11,12]

Analyses were performed using Statcel (OMS, Saitama, Japan), StatView ver 5.0 (SAS Institute, Cary, NC, USA), and Deltagraph 5.4.5v J (Deltapoint, Monterey, CA, USA) software. Values in the text are expressed as the mean ± standard deviation (SD) unless otherwise noted. The Z of r and RMS values were compared between the goodness of h-L and m-E fits. The Student's paired t test was used for comparison between h-L and m-E Z and Wilcoxon signed-rank test was used for comparison between h-L and m-E RMS. Simple linear regression analyses were performed between the h-L amplitude constants and between the h-L time constants for the different partial phases of CaTC. A p value of < 0.05 was considered to indicate statistical significance.

RESULTS

h-L and m-E curve-fits

Four observed CaTCIIIs, in which both the absolute

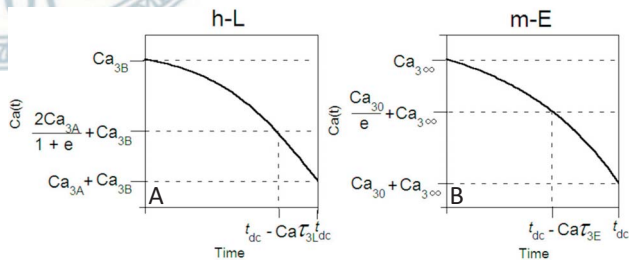

Figure 2. *Half-logistic (h-L) and mono-exponential (m-E) distribution function curves for the observed first half of the descending phase of the cardiomyocyte cytoplasmic Ca^{2+} concentration ($[Ca^{2+}]_i$)-time curve (CaTCIII). (A) The h-L function curve described in Equation 1 (see text). Ca_{3A}, h-L amplitude constant of CaTCIII; $Ca\tau_{3L}$, h-L time constant of CaTCIII; Ca_{3B}, h-L non-zero asymptote of CaTCIII; t_{dC}, time at the point corresponding to the minimum of the first-order time derivative of the $[Ca^{2+}]_i$ (dCa/dt_{min}) data. (B) The m-E function curve described in Equation 2. Ca_{30}, m-E amplitude constant of CaTCIII; $Ca\tau_{3E}$, m-E time constant of CaTCIII; $Ca_{3\infty}$, m-E non-zero asymptote of CaTCIII.*

Ca_{3A} and the absolute Ca_{30} were larger than the peak $[Ca^{2+}]_i$, could not be appropriately curve-fitted by the h-L and m-E functions, and were deleted from the analysis. The observed values of the remaining 11 CaTCIIIs are shown in Table 1. The time during the 11 observed CaTCIIIs was 23.8 ± 8.9 ms and the number of the observed $[Ca^{2+}]_i$ data used for analysis was 24.8 ± 8.9 points. The three h-L and m-E function parameters curve-fitted for the observed $[Ca^{2+}]_i$ data during the 11 CaTCIIIs are shown in Table 2.

The representative best-fitted h-L and m-E function curves for the observed $[Ca^{2+}]_i$ data during CaTCIII in the muscle of a mouse are shown in Figure 3A and B, respectively. The residual Ca^{2+} concentrations, calculated from the observed $[Ca^{2+}]_i$ data during CaTCIII minus the best-fitted h-L and m-E curves, are shown in Figure 3C and D, respectively.

Goodness of h-L and m-E fits

The mean *r* values of the h-L and m-E functions, curve-fitted for the observed $[Ca^{2+}]_i$ data during the 11 CaTCIIIs, were 0.9986 and 0.9982, respectively. The Fisher's *Z* transformation values of the 11 h-L *r* and m-E function *r* were 3.64 ± 0.45 and 3.50 ± 0.33, respectively. The h-L *Z* transformation value was significantly larger than the m-E *Z* transformation value ($p < 0.05$).

The RMS values of the h-L and m-E function best curve-fits for 11 CaTCIIIs were 63.6 ± 71.9 and 67.9 ± 69.7 $(nmol/l)^2$, respectively. The h-L RMS tended to be smaller than the m-E RMS, but was not significantly so.

DISCUSSION

These results demonstrated that the h-L function can curve-fit most CaTCIIIs more accurately than the m-E function in isolated aequorin-injected mouse LV papillary muscles. Therefore, we suggest that three calculated h-L function parameters i.e., Ca_{3A}, $Ca\tau_{3L}$, and Ca_{3B}, can be used to more reliably characterize the magnitude and time course of CaTCIII.

Myocardial Ca^{2+} handling

During a cardiac cycle, the contraction process causes Ca^{2+} inflow into the cardiomyocyte cytoplasm through voltage-dependent sarcolemmal (SL) L-type Ca^{2+} channels (LCC) and release of Ca^{2+} from the ryanodine receptor (RyR) of SR, induced by Ca^{2+} influx through SL LCC and the sensitivity of myofilaments to Ca^{2+}. Most Ca^{2+} flows into the cytoplasm from the RyR of SR by CICR, with only a small amount of Ca^{2+} flowing into the cytoplasm through LCC. During each heartbeat, a transient increase in the myocardial $[Ca^{2+}]_i$ induces a transient increase in the binding of Ca^{2+} to a major Ca^{2+}-binding protein, troponin C (TnC), and a transient increase in the attachment of the thick-filament myosin cross-bridge (CB) to thin-filament actin, which precedes and initiates myocardial contraction and an increase in LV pressure.

Table 1. Observed values of the cardiomyocyte cytoplasmic Ca^{2+} concentration ($[Ca^{2+}]_i$)-time curve (CaTC)

	Observed value
$[Ca^{2+}]_i$ at dCa/dt_{max} (nmol/l)	846 ± 201
Peak $[Ca^{2+}]_i$ (nmol/l)	1,776 ± 364
$[Ca^{2+}]_i$ at dCa/dt_{min} (nmol/l)	1,424 ± 396
Time to dCa/dt_{max} (ms)	59.9 ± 1.3
Time to peak $[Ca^{2+}]_i$ (ms)	76.9 ± 1.8
Time to dCa/dt_{min} (ms)	100.7 ± 9.0
dCa/dt_{max} (nmol/l/ms)	124.6 ± 30.0
dCa/dt_{min} (nmol/l/ms)	-21.6 ± 4.7

Data are presented as the mean ± standard deviation (SD) of the observed values of CaTCs in the 11 isolated mouse aequorin-injected left ventricular (LV) papillary muscles. dCa/dt_{max}, maximum of the first-order time derivative of $[Ca^{2+}]_i$; dCa/dt_{min}, minimum of the first-order time derivative of $[Ca^{2+}]_i$.

Table 2. Three calculated half-logistic (h-L) and mono-exponential (m-E) function parameters for the observed first half of the descending phase of the cardiomyocyte cytoplasmic Ca^{2+} concentration ($[Ca^{2+}]_i$)-time curve (CaTCIII)

h-L		m-E	
Ca_{3A}	-527 ± 266 nmol/l	Ca_{30}	-872 ± 631 nmol/l
$Ca\tau_{3L}$	14.2 ± 9.2 ms	$Ca\tau_{3E}$	44.3 ± 38.7 ms
Ca_{3B}	1,954 ± 368 nmol/l	$Ca_{3\infty}$	2,295 ± 608 nmol/l

Data are presented as the mean ± standard deviation (SD) of the calculated values of the h-L and m-E function parameters for the CaTCIIIs in the 11 isolated mouse aequorin-injected left ventricular (LV) papillary muscles. Ca_{3A}, h-L amplitude constant of CaTCIII; $Ca\tau_{3L}$, h-L time constant of CaTCIII; Ca_{3B}, h-L non-zero asymptote of CaTCIII; Ca_{30}, m-E amplitude constant of CaTCIII; $Ca\tau_{3E}$, m-E time constant of CaTCIII; $Ca_{3\infty}$, m-E non-zero asymptote of CaTCIII.

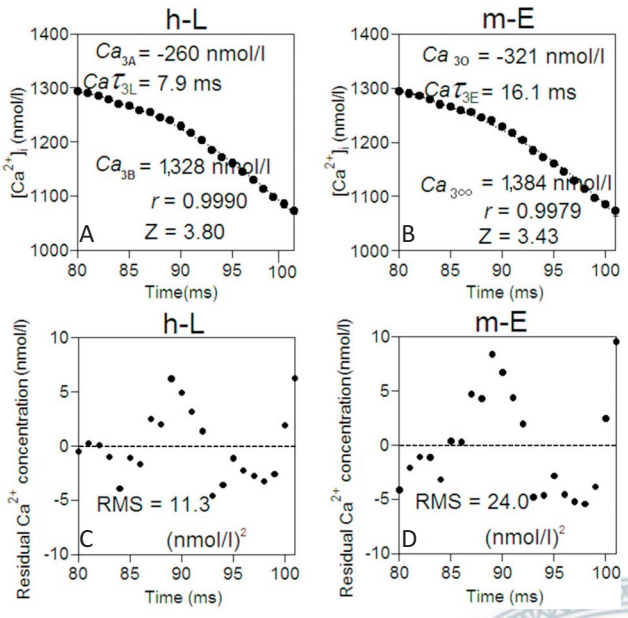

Figure 3. *Representative best-fitted half-logistic (h-L) and mono-exponential (m-E) function curves for the observed first half of the descending phase of the cardiomyocyte cytoplasmic Ca^{2+} concentration ($[Ca^{2+}]_i$)-time curve (CaTCIII) data in the interval from the point corresponding to the peak $[Ca^{2+}]_i$ data to the point corresponding to the minimum of the first-order time derivative of $[Ca^{2+}]_i$ (dCa/dt_{min}) data at 0.5 Hz beating frequency in the isolated aequorin-injected left ventricular (LV) papillary muscle of a mouse. (A) Representative best-fitted h-L function curve (thin line) for the observed $[Ca^{2+}]_i$ data during CaTCIII (dots). Ca_{3A}, h-L amplitude constant of CaTCIII; $Ca\tau_{3L}$, h-L time constant of CaTCIII; Ca_{3B}, h-L non-zero asymptote of CaTCIII; r, correlation coefficient; Z, Fisher's Z transformation of r. (B) Representative best-fitted m-E function curve (thin line) for the observed $[Ca^{2+}]_i$ data during CaTCIII (dots). Ca_{3O}, m-E amplitude constant of CaTCIII; $Ca\tau_{3E}$, m-E time constant of CaTCIII; $Ca_{3\infty}$, m-E non-zero asymptote of CaTCIII. (C) Residual Ca^{2+} concentrations (dots) calculated from the observed $[Ca^{2+}]_i$ data during CaTCIII minus the best-fitted h-L curve shown in (A). RMS, residual mean square. (D) Residual Ca^{2+} concentrations (dots) calculated from the observed $[Ca^{2+}]_i$ data during CaTCIII minus the best-fitted m-E curve shown in (B).*

Because myocardial contraction lags behind the increase in $[Ca^{2+}]_i$, the magnitude of the contraction is determined not only by the magnitude of $[Ca^{2+}]_i$ but also by its duration. Thereafter, myocardial relaxation lags behind the decrease in $[Ca^{2+}]_i$. The relaxation process involves Ca^{2+} dissociation from TnC, Ca^{2+} sequestration into SR, and Ca^{2+} removal from the cytoplasm to the extracellular space through the Na^+/Ca^{2+} exchanger.

Waveform analysis for four partial CaTCs

CaTC is expected to change in tandem with the magnitudes and time courses of the myocardial force-time curve (FTC) and LV pressure-time curve (PTC). We have reported that the h-L function outperforms the m-E function in curve-fitting the following: (i) the first half of the descending phase of the isometric FTC (FTCIII) in the interval from the point corresponding to the peak tension to the point corresponding to the minimum of the first-order time derivative of tension (dF/dt_{min}) in the myocardial muscle,[13] and (ii) the first half of the descending phase of the isovolumic LV PTC (PTCIII) in the interval from the point corresponding to the peak LV pressure to the point corresponding to the minimum of the first-order time derivative of LV pressure (dP/dt_{min}) in the cross-circulated dog heart.[14]

The calculated function parameters were used to summarize the waveforms of four partial phases of the observed CaTC with almost no loss of information on the characteristics. The m-E function has been used for curve-fitting CaTCI,[2] CaTCII,[3] and CaTCIV[4] in the papillary muscles of mice and rabbits, and CaTCIV in the isovolumic LV in excised whole hearts of rats,[15-17] and in cardiomyocytes of mice,[18-20] rabbits,[19-21] rats,[21-23] dogs,[19] and humans.[19] It is known that duration of CICR, activity of the SR Ca^{2+}-ATPase, and activity of Na^+/K^+ exchanger are dependent on animal species. For example, there are significant differences in the m-E time constant of CaTCIV ($Ca\tau_{4E}$), reflecting the activities of the SR Ca^{2+}-ATPase, with values for cardiomyocytes decreasing in the order of humans, dogs, rabbits, and mice.[19]

Magnitude during CaTCIII

Three calculated h-L function parameters curve-fitted for CaTCIII were able to summarize the magnitude and time course, with almost no loss of information on the characteristics of the observed CaTCIII. Three calculated h-L function parameters may have physiological as well as mathematical meanings.

The Ca_{3A} and Ca_{3B} have physiological and mathematical meanings. The absolute value of Ca_{3A} represents the difference between the peak $[Ca^{2+}]_i$ and $[Ca^{2+}]_i$ at the point corresponding to the minimum rate of decrease in $[Ca^{2+}]_i$ i.e., dCa/dt_{min}, as shown in Figure 2A. The Ca_{3A} plus Ca_{3B} value represents Ca^{2+} concentration at the point corresponding to the peak $[Ca^{2+}]_i$.

There were no significant relationships between the h-L amplitude constant of CaTCI (Ca_{1A}) and the absolute value of Ca_{3A}, between the absolute value of the h-L am-

plitude constant of CaTCII (Ca_{2A}) and the absolute value of Ca_{3A}, and between the h-L amplitude constant of CaTCIV (Ca_{4A}) and the absolute value of Ca_{3A} for the 11 CaTCs (see APPENDIX). However, there were significant relationships between Ca_{1A} and Ca_{4A}. Moreover, in the previous study, we demonstrated significant relationships between Ca_{1A} and the absolute value of Ca_{2A}, and between Ca_{4A} and the absolute value of Ca_{2A}.[3]

These results show that the magnitude of CaTCIII does not relate to that of CaTCI, CaTCII, or CaTCIV, among which, however, there are good relationships.

Time course during CaTCIII

The $Ca\tau_{3L}$ has physiological and mathematical meanings. The $Ca\tau_{3L}$ represents the time from 2/(1 + e) of Ca_{3A} plus Ca_{3B} to Ca_{3A} plus Ca_{3B}, as shown in Figure 2A.

The time constants for four partial phases of the observed CaTC are used for comparison of the duration (see APPENDIX). The $Ca\tau_{3L}$ was significantly longer than $Ca\tau_{1L}$ and the h-L time constant of CaTCII ($Ca\tau_{2L}$) ($p < 0.005$), and significantly shorter than $Ca\tau_{4L}$ ($p < 0.0005$), tested using the Student's paired *t* test.

There was a significant negative correlation between $Ca\tau_{4L}$ and $Ca\tau_{3L}$ (see APPENDIX). This supports the assertion that $Ca\tau_{3L}$ is dependent on $Ca\tau_{4L}$. CaTCIII corresponds to the combination of the last phase of the increase in cardiomyocyte cytoplasmic Ca^{2+} concentration from SR by CICR, and the middle phase of the decrease in cytoplasmic Ca^{2+} concentration by Ca^{2+} sequestration into SR and Ca^{2+} removal from the cytoplasm to the extracellular space through the Na^+/Ca^{2+} exchanger. CaTCIII includes both the late part of the contraction process and the middle part of the relaxation process, and represents the change in the difference between the Ca^{2+} inflow into cytoplasm and the Ca^{2+} outflow from it, although the degree of the Ca^{2+} outflow from the cytoplasm is larger than that of the Ca^{2+} inflow into it. Accordingly, $Ca\tau_{3L}$ evaluates the duration of the change in the decrease in $[Ca^{2+}]_i$. Furthermore, we have established a tendency toward a slight negative correlation between $Ca\tau_{2L}$ and $Ca\tau_{4L}$. We suggest that the change in $[Ca^{2+}]_i$ during CaTCIV with the simple relaxation process influences the changes in $[Ca^{2+}]_i$ during CaTCII with the combination of the middle part of the contraction process and the early part of the relaxation process, and CaTCIII, with the combination of the late part of the contraction process and middle part of the relaxation process. Therefore, the faster speed of the relaxation process may more strongly decrease CaTCIII after the peak $[Ca^{2+}]_i$.

However, there were no significant relationships between $Ca\tau_{1L}$ and $Ca\tau_{3L}$, between $Ca\tau_{2L}$ and $Ca\tau_{3L}$, and between $Ca\tau_{1L}$ and $Ca\tau_{4L}$. In the previous study, we demonstrated that there were no significant relationships between $Ca\tau_{1L}$ and $Ca\tau_{2L}$.[3] These results support the assertion that $Ca\tau_{3L}$ is independent of $Ca\tau_{1L}$ and $Ca\tau_{2L}$. Taken together, these data indicate that the time course in the change in $[Ca^{2+}]_i$ during CaTCIII is different from that of CaTCI and CaTCII. These results indicate that each phase has its own time constant, and there may be individual differences in Ca^{2+} handling, such as Ca^{2+} flow into the cardiomyocyte cytoplasm from SR by CICR during the contraction process, Ca^{2+} sequestration into SR, and Ca^{2+} removal from the cytoplasm to the extracellular space through the Na^+/Ca^{2+} exchanger during the relaxation process. It may be possible to obtain significant insight into each process in myocardial Ca^{2+} handling and E-C coupling by using each h-L time constant.

The three calculated h-L function parameters enable the comparison between the magnitudes and time courses of the four phases of the observed CaTC. Curve-fitting for each phase by the h-L function would be useful for studying the effect of $[Ca^{2+}]_i$ during each process in myocardial Ca^{2+} handling.

Sigmoid logistic function

The logistic function has been widely used to study rising phenomena in many fields of bioscience and to intuitively describe symmetrical sigmoid curves whose inflection point corresponds to a boundary, such as those found in mortality/survival curves[24] and growth curves.[25,26] The logistic nature of these phenomena predicts that the process is initially minimal, increases gradually, and maximizes to an upper asymptote: conversely, it is initially maximal, decreases gradually, and minimizes to a lower asymptote. The logistic function is limited in its ability to represent the symmetrical sigmoid function, especially as it reaches the upper or lower asymptote.

In comparison, the m-E function is used to model phenomena when a constant change in the independent variable gives the same proportional change. The graph

of the m-E function indicates when a quantity increases or decreases at a rate proportional to its current value.

In a previous study, we reported that the sigmoid logistic function satisfactorily curve-fits the entire ascending phase in the duration from the point corresponding to the beginning of twitch stimulation to the point corresponding to the peak $[Ca^{2+}]_i$ and the entire descending phase in the interval from the point corresponding to the peak $[Ca^{2+}]_i$ to the point corresponding to the resting $[Ca^{2+}]_i$.[27] Computer simulation of the $[Ca^{2+}]_i$ transient also provided a characterization of the sigmoid logistic function.[28]

Curve-fitting for the entire ascending phase and the entire descending phase of the observed CaTC data by the sigmoid logistic function would be useful for evaluating dCa/dt_{max} and dCa/dt_{min}, respectively. However, in the previous study we found that the entire ascending phase of the observed CaTC data is asymmetrical at the point corresponding to dCa/dt_{max}.[3] Moreover, in the present study we found that the entire descending phase of the observed CaTC data is asymmetrical at the point corresponding to dCa/dt_{min}.

Study limitations

There are several limitations of this study. First, the experimental condition used to measure $[Ca^{2+}]_i$ was not physiological i.e., 100% L_{max} with 2-mM extracellular Ca^{2+} at 30 °C and a stimulation frequency of 0.2 Hz. Further examination of these concepts is needed under different physiological conditions of preloads, extracellular Ca^{2+} concentrations, temperatures, stimulation frequencies, and pharmacological conditions with varying degrees of blocking or stimulating agents of channels, pumps, exchangers, β-adrenergic receptor agonists (e.g., isoproterenol[29]), cardiac glycoside (e.g., dihydroouabain[29]), Ca^{2+}-store depleting agents (e.g., ryanodine[30]), and anesthetic agents (e.g., sevoflurane[31]). Moreover, it will be beneficial if future studies include a pathological model, such as dilated cardiomyopathy, hypertrophic cardiomyopathy, and ischemic heart failure, to demonstrate correlations of h-L function parameters with changes in Ca^{2+} regulation proteins. Furthermore, this method may also be applied in other animal species or atria. Second, we used the Ca^{2+}-sensitive photoprotein aequorin, which is a good indicator of the change in $[Ca^{2+}]_i$. Additional investigations with other Ca^{2+}-sensitive fluorescent indicators, such as indo-1, rhod-2, fura-2, and fluo-3, would be useful. Third, we curve-fitted CaTCIII using the h-L function model with three variable parameters. We intend to develop the h-L function with an additional variable parameter or a new function to curve-fit it more accurately.

In the present study, four of the 15 CaTCIIIs could not be curve-fitted appropriately by h-L and m-E functions. The $Ca\tau_{3L}$ value was too much longer and the Ca_{3B} value was too much larger than the corresponding values for the observed CaTCIII. Because the four CaTCIIIs may be straight rather than convex, the inflexion point of the entire descending phase could not be identified. The degree of the relaxation process during the four CaTCIIIs may be stronger, and $[Ca^{2+}]_i$ may decrease rapidly. In addition, the SD values of three calculated h-L function parameters for the 11 CaTCIIIs are larger than those for the 11 CaTCIs, CaTCIIs, and CaTCIVs. The asymptote of CaTCIII i.e., dCa/dt = 0 nmol/l/ms is only one point, and CaTCI and CaTCIV have longer asymptotes. The magnitudes and time courses during CaTCIII, which means the combination of the late part of the contraction process and the middle part of the relaxation process, may be dependent on Ca^{2+} handling in each mammalian cardiac muscle. Further examination is needed to determine the location of the inflexion point of the entire descending phase and understand Ca^{2+} handling during CaTCIII.

CONCLUSIONS

The h-L functions can evaluate most of CaTCIIIs more accurately than the m-E functions in isolated aequorin-injected mouse LV papillary muscles. The absolute values of Ca_{3A}, $Ca\tau_{3L}$, and Ca_{3B} are more reliable indices for evaluating the magnitude and time course of the change in the decrease in $[Ca^{2+}]_i$ during CaTCIII. The h-L approach may provide a more useful model for the study of each process in myocardial Ca^{2+} handling.

ACKNOWLEDGEMENTS

We would like to gratefully thank Drs. Shuta Hirano, Yoichiro Kusakari, and Satoshi Kurihara at the Department of Cell Physiology, The Jikei University School of Medicine, for their excellent research assistance.

REFERENCES

1. Kurihara S. Regulation of cardiac muscle contraction by intracellular Ca^{2+}. *Jpn J Physiol* 1994;44:591-611.
2. Mizuno J, Hanaoka K, Otsuji M, et al. Calcium-induced calcium release from the sarcoplasmic reticulum can be evaluated with a half-logistic function model in aequorin-injected cardiac muscles. *J Anesth* 2011;25:831-9.
3. Mizuno J, Otsuji M, Hanaoka K, et al. Intracellular Ca^{2+} transient Phase II can be assessed by half-Logistic function model in isolated aequorin-injected mouse left ventricular papillary muscle. *Acta Cardiol Sin* 2013;29:328-38.
4. Mizuno J, Otsuji M, Takeda K, et al. Superior logistic model for decay of Ca^{2+} transient and isometric relaxation force curve in rabbit and mouse papillary muscles. *Int Heart J* 2007;48:215-32.
5. Allen DG, Kurihara S. The effects of muscle length on intracellular calcium transients in mammalian cardiac muscle. *J Physiol* 1982; 327:79-94.
6. Hirano S, Kusakari Y, O-Uchi J, et al. Intracellular mechanism of the negative inotropic effect induced by α1-adrenoceptor stimulation in mouse myocardium. *J Physiol Sci* 2006;56:297-304.
7. Ishikawa T, Mochizuki S, Kurihara S. Cross-bridge-dependent change of the Ca^{2+} sensitivity during relaxation in aequorin-injected tetanized ferret papillary muscles. *Circ J* 2006;70:913-8.
8. Allen DG, Blinks JR, Prendergast FG. Aequorin luminescence: relation of light emission to calcium concentration-a calcium-independent component. *Science* 1977;195:996-8.
9. Okazaki O, Suda N, Hongo K, et al. Modulation of Ca^{2+} transients and contractile properties by β-adrenoceptor stimulation in ferret ventricular muscles. *J Physiol* 1990;423:221-40.
10. Snedecor GW, Cochran WG. *Statistical methods* (6th edition). Iowa State University Press, Ames, Iowa, 1971:185.
11. Thompson DS, Waldron CB, Coltart DJ, et al. Estimation of time constant of left ventricular relaxation. *Br Heart J* 1983;49:250-8.
12. Thompson DS, Wilmshurst P, Juul SM, et al. Pressure-derived indices of left ventricular isovolumic relaxation in patients with hypertrophic cardiomyopathy. *Br Heart J* 1983;49:259-67.
13. Mizuno J, Morita S, Otsuji M, et al. Half-logistic time constants as inotropic and lusitropic indices for four sequential phases of isometric tension curves in isolated rabbit and mouse papillary muscles. *Int Heart J* 2009;50:389-404.
14. Mizuno J, Shimizu J, Mohri S, et al. Hypovolemia does not affect speed of isovolumic left ventricular contraction and relaxation in excised canine heart. *Shock* 2008;29:395-401.
15. Camacho SA, Brandes R, Figueredo VM, et al. Ca^{2+} transient decline and myocardial relaxation are slowed during low flow ischemia in rat hearts. *J Clin Invest* 1994;93:951-7.
16. Chang KC, Schreur JH, Weiner MW, et al. Impaired Ca^{2+} handling is an early manifestation of pressure-overload hypertrophy in rat hearts. *Am J Physiol* 1996;271:H228-34.
17. Halow JM, Figueredo VM, Shames DM, et al. Role of slowed Ca^{2+} transient decline in slowed relaxation during myocardial ischemia. *J Mol Cell Cardiol* 1999;31:1739-48.
18. Lim CC, Apstein CS, Colucci WS, et al. Impaired cell shortening and relengthening with increased pacing frequency are intrinsic to the senescent mouse cardiomyocyte. *J Mol Cell Cardiol* 2000; 32:2075-82.
19. Su Z, Li F, Spitzer KW, et al. Comparison of sarcoplasmic reticulum Ca^{2+}-ATPase function in human, dog, rabbit, and mouse ventricular myocytes. *J Mol Cell Cardiol* 2003;35:761-7.
20. Su Z, Sugishita K, Li F, et al. Effects of FK506 on $[Ca^{2+}]_i$ differ in mouse and rabbit ventricular myocytes. *J Pharmacol Exp Ther* 2003;304:334-41.
21. Bassani JWM, Bassani RA, Bers DM. Relaxation in rabbit and rat cardiac cells: species-dependent differences in cellular mechanisms. *J Physiol* 1994;476:279-93.
22. Bers DM, Berlin JR. Kinetics of $[Ca]_i$ decline in cardiac myocytes depend on peak $[Ca]_i$. *Am J Physiol* 1995;268:C271-7.
23. Brittsan AG, Ginsburg KS, Chu G, et al. Chronic SR Ca^{2+}-ATPase inhibition causes adaptive changes in cellular Ca^{2+} transport. *Circ Res* 2003;92:769-76.
24. Wilson DL. The analysis of survival (mortality) data: fitting Gompertz, Weibull, and logistic functions. *Mech Ageing Dev* 1994; 74:15-33.
25. Sheehy JE, Mitchell PL, Ferrer AB. Bi-phasic growth patterns in rice. *Ann Bot (Lond)* 2004;94:811-7.
26. Fujikawa H, Morozumi S. Modeling surface growth of escherichia coli on agar plates. *Appl Environ Microbiol* 2005;71:7920-6.
27. Mizuno J, Otsuji M, Arita H, et al. Characterization of intracellular Ca^{2+} transient by the hybrid logistic function in aequorin-injected rabbit and mouse papillary muscles. *J Physiol Sci* 2007;57:349-59.
28. Sakamoto T, Matsubara H, Hata Y, et al. Logistic character of myocardial twitch force curve: simulation. *Heart Vessel* 1996;11: 171-9.
29. Hotta Y, Ando H, Fujita M, et al. Different effects of isoproterenol and dihydroouabain on cardiac Ca2+ transients. *Eur J Pharmacol* 1995;282:121-30.
30. Wu SN, Shen AY, Hwang TL. Analysis of mechanical restitution and post-rest potentiation in isolated rat atrium. *Clin J Physiol* 1996;39:23-9.
31. Bartunek AE, Housmans PR. Effects of sevoflurane on the intracellular Ca^{2+} transient in ferret cardiac muscle. *Anesthesiology* 2000;93:1500-8.

APPENDIX

The following h-L function is used to curve-fit CaTCI data, which extends from the point corresponding to the beginning of twitch stimulation to the point corresponding to the dCa/dt_{max} data, shown in Figure 1 by the least-squares method:

$$Ca(t) = 2Ca_{1A}/\{1 + \exp[-(t - t_{aC})/Ca\tau_{1L}]\} + Ca_{1B} \quad \text{(Eq. 3)}$$

where t is the time from the point corresponding to the beginning of twitch stimulation to the $[Ca^{2+}]_i$, Ca_{1A} is the h-L amplitude constant of CaTCI, $Ca\tau_{1L}$ is the h-L time constant of CaTCI, Ca_{1B} is the h-L non-zero asymptote of CaTCI, and t_{aC} is a constant which represents the time at the point corresponding to dCa/dt_{max}.[2] It is noted that t_{aC} is determined before the function h-L curve fitting. The h-L function curve given by Eq. 3 increases monotonically from Ca(0) (= Ca_{1B}) to $Ca(t_{aC})$ [= (Ca_{1A} + Ca_{1B})]. The $Ca\tau_{1L}$ value corresponds to the duration for the curves to increase from $Ca(t_{aC} - Ca\tau_{1L})$ {= [$2Ca_{1A}/(1 + e)$ + Ca_{1B}] ~ (0.54 Ca_{1A} + Ca_{1B})} to $Ca(t_{aC})$ [= (Ca_{1A} + Ca_{1B})]. The Ca_{1A}, $Ca\tau_{1L}$, and Ca_{1B} values curve-fitted for the 11 CaTCIs were 898 ± 215 nmol/l, 2.2 ± 0.2 ms, and 1.5 ± 6.4 nmol/l, respectively. The mean r value was 0.9901.

The following h-L function is used to curve-fit CaTCII data, which extends from the point corresponding to dCa/dt_{max} to the point corresponding to the peak $[Ca^{2+}]_i$ data, shown in Figure 1 by the least-squares method:

$$Ca(t) = 2Ca_{2A}/\{1 + \exp[(t - t_{aC})/Ca\tau_{2L}]\} + Ca_{2B} \quad \text{(Eq. 4)}$$

where t is the time from the point corresponding to twitch stimulation to the point corresponding to the $[Ca^{2+}]_i$, Ca_{2A} is the h-L amplitude constant of CaTCII, $Ca\tau_{2L}$ is the h-L time constant of CaTCII, Ca_{2B} is the h-L non-zero asymptote of CaTCII, and t_{aC} is a constant which represents the time at the point corresponding to dCa/dt_{max}.[3] It is noted that t_{aC} is determined before the h-L function curve fitting. The h-L function curve given by Eq. 4 increases monotonically from $Ca(t_{aC})$ [= (Ca_{2A} + Ca_{2B})] to Ca(∞) [= Ca_{2B}]. The $Ca\tau_{2L}$ value corresponds to the duration for the curves to increase from $Ca(t_{aC})$ [= (Ca_{2A} + Ca_{2B})] to $Ca(t_{aC} + Ca\tau_{2L})$ {= [$2Ca_{2A}/(1 + e)$ + Ca_{2B}] ~ (0.54 Ca_{2A} + Ca_{2B})}. The Ca_{2A}, $Ca\tau_{2L}$, and Ca_{2B} values curve-fitted for the 11 CaTCIIs were -974 ± 223 nmol/l, 3.8 ± 0.5 ms, and 1,816 ± 375 nmol/l, respectively. The mean r value was 0.9997.

The following h-L function is used to curve-fit CaTCIV data, which extends from the point corresponding to dCa/dt_{min} data to the point corresponding to the resting $[Ca^{2+}]_i$ data, shown in Figure 1 by the least-squares method:

$$Ca(t) = 2Ca_{4A}/\{1 + \exp[(t - t_{dC})/Ca\tau_{4L}]\} + Ca_{4B} \quad \text{(Eq. 5)}$$

where t is the time from the point corresponding to twitch stimulation to the point corresponding to the $[Ca^{2+}]_i$, Ca_{4A} is the h-L amplitude constant of CaTCIV, $Ca\tau_{4L}$ is the h-L time constant of CaTCIV, Ca_{4B} is the h-L non-zero asymptote of CaTCIV, and t_{dC} is a constant which represents the time at the point corresponding to dCa/dt_{min}.[4] It is noted that t_{dC} is determined before the h-L function curve fitting. The h-L function curve given by Eq. 5 decreases monotonically from $Ca(t_{dC})$ [= (Ca_{4A} + Ca_{4B})] to Ca(∞) [= Ca_{4B}]. The $Ca\tau_{4L}$ value corresponds to the duration for the curves to decrease from $Ca(t_{dC})$ [= (Ca_{4A} + Ca_{4B})] to $Ca(t_{dC} + Ca\tau_{4L})$ {= [$2Ca_{4A}/(1 + e)$ + Ca_{4B}] ~ (0.54 Ca_{4A} + Ca_{4B})}. The Ca_{4A}, $Ca\tau_{4L}$, and Ca_{4B} values curve-fitted for the 11 CaTCIVs were 1,419 ± 389 nmol/l, 38.7 ± 5.2 ms, and -0.5 ± 12.7 nmol/l, respectively. The mean r value was 0.9974.

Simple linear regression formulas between the calculated h-L amplitude constants were following; Absolute value of Ca_{3A} = 0.03 Ca_{1A} + 0.50 (r = 0.02, p = 0.94). Absolute value of Ca_{3A} = -0.39 Ca_{2A} + 0.91 (r = 0.33, p = 0.32). Absolute value of Ca_{3A} = - 0.32 Ca_{4A} + 0.98 (r = 0.47, p = 0.15). Ca_{4A} = 1.40 Ca_{1A} + 0.16 (r = 0.78, p = 0.005).

Simple linear regression formulas between the calculated h-L time constants were following; $Ca\tau_{3L}$ = -0.81 $Ca\tau_{1L}$ + 16.08 (r = 0.01, p = 0.97). $Ca\tau_{3L}$ = 5.94 $Ca\tau_{2L}$ − 8.44 (r = 0.32, p = 0.34). $Ca\tau_{3L}$ = -1.15 $Ca\tau_{4L}$ + 58.66 (r = 0.65, p = 0.03). $Ca\tau_{4L}$ = -15.52 $Ca\tau_{1L}$ + 72.93 (r = 0.47, p = 0.14).